Cureus
Part of SPRINGER NATURE

Open Access Case Report

Giant Paratesticular Leiomyosarcoma Mimicking a Benign Paratesticular Neoplasm: Multimodality Imaging and Radiologic-Pathologic Correlation

Anvay Pangaonkar [1], Pratiksha Sachani [2], Suresh Phatak [2], Kajal Mitra [3], Prashant Onkar [2]

1. Radiology, NKP Salve Institute of Medical Sciences and Lata Mangeshkar Hospital, Nagpur, IND 2. Radiodiagnosis, NKP Salve Institute of Medical Sciences and Lata Mangeshkar Hospital, Nagpur, IND 3. Radiodiagnosis and Imaging, NKP Salve Institute of Medical Sciences and Lata Mangeshkar Hospital, Nagpur, IND

Corresponding author: Anvay Pangaonkar, anvayp9@gmail.com

Review began 10/26/2026
Review ended 11/06/2026
Published 11/09/2026

© **Copyright** 2026
Pangaonkar et al. This is an open access article distributed under the terms of the Creative Commons Attribution License CC-BY 4.0., which permits unrestricted use, distribution, and reproduction in any medium, provided the original author and source are credited.

DOI: 10.7759/cureus.119349

Abstract

Paratesticular leiomyosarcoma is an uncommon malignant mesenchymal tumor with nonspecific imaging features that may overlap with benign paratesticular neoplasms. We report the case of a 46-year-old man presenting with progressive enlargement of the right hemiscrotum over six months. Ultrasonography demonstrated a large, well-defined heterogeneous solid-cystic paratesticular mass with a separately visualized testis and no significant internal Doppler vascularity. CT confirmed a large heterogeneous right scrotal/paratesticular mass with inferior displacement of the testis. MRI demonstrated a 14.6 × 11.1 × 10.5 cm well-defined solid-cystic lesion with T1-hypointense and T2/short tau inversion recovery-hyperintense signal, scattered hypointense solid components, delayed enhancement, prominent tortuous intralesional vessels on susceptibility-weighted imaging, and no convincing diffusion restriction. The imaging appearance favored a benign paratesticular neoplasm, with cellular angiofibroma and epididymal leiomyoma considered the principal differential diagnoses. Radical orchiectomy yielded an 850-g mass measuring 18.5 × 11.3 × 9.3 cm. Histopathological examination demonstrated a circumscribed spindle-cell neoplasm arranged predominantly in fascicles, confirming leiomyosarcoma. Immunohistochemistry showed positivity for smooth muscle actin and desmin, with a Ki-67 proliferation index of approximately 10%. The tumor demonstrated 8 mitoses per 10 high-power fields, with no tumor necrosis, and was classified as French Federation of Cancer Centers Sarcoma Group Grade 1 (total score: 3). This case highlights that a very large paratesticular leiomyosarcoma can retain well-defined margins and lack convincing diffusion restriction, thereby mimicking a benign lesion. Accurate localization, multimodality assessment, and radiologic-pathologic correlation are important when evaluating a large or progressively enlarging paratesticular mass.

Categories: Urology, Radiology, Pathology
Keywords: epididymis, extratesticular tumor, magnetic resonance imaging, paratesticular leiomyosarcoma, radiologic–pathologic correlation, scrotal mass, ultrasonography

Introduction

Paratesticular tumors arise from structures external to the testicular parenchyma, including the epididymis, spermatic cord, tunical structures, and surrounding soft tissues. Most paratesticular masses are benign, whereas malignant lesions are predominantly sarcomas; leiomyosarcoma is an uncommon adult paratesticular sarcoma [1-3].

Paratesticular leiomyosarcoma may arise from smooth muscle elements of the spermatic cord, epididymis, tunica, or scrotal soft tissues. Epididymal involvement is particularly uncommon, with a limited number of reported cases [1,4,5]. A systematic review of epididymal leiomyosarcoma identified 13 reported cases, underscoring the rarity of this entity [4].

Ultrasonography is the initial imaging examination for most scrotal masses and is particularly useful for establishing whether a lesion is intratesticular or extratesticular. MRI provides superior soft-tissue characterization and assessment of local relationships, whereas CT is primarily useful for staging and assessment of regional or distant disease [2,3]. However, substantial imaging overlap exists between benign and malignant paratesticular neoplasms.

Case Presentation

Clinical presentation

A 46-year-old man presented with a six-month history of progressively enlarging right hemiscrotal swelling. Clinical examination revealed a large, firm, non-tender right scrotal swelling occupying the right hemiscrotum. The overlying scrotal skin appeared normal. The right testis could not be palpated satisfactorily due to the size of the swelling. The ability to get above the swelling was preserved. Cough

impulse was negative, and the transillumination test was negative. There was no documented history of fever or preceding trauma, and the available clinical records did not reveal significant associated urinary or gastrointestinal symptoms. In view of the progressive enlargement of the right hemiscrotum, firm consistency of the swelling, inability to palpate the right testis separately, and negative transillumination test, a provisional clinical diagnosis of a right testicular mass was made. Although the initial clinical assessment raised suspicion of a testicular mass, the precise anatomical origin of the lesion could not be established clinically. Its paratesticular origin was assigned retrospectively following radiological evaluation, which demonstrated the right testis separately from the mass. Serum tumor markers, including alpha-fetoprotein (AFP), beta-human chorionic gonadotropin (β-hCG), and lactate dehydrogenase (LDH), were subsequently assessed as part of the initial evaluation. The results revealed serum AFP of 2 ng/mL, β-hCG of 1.2 mIU/mL, and LDH of 150 U/L, all within their respective normal reference ranges.

Imaging findings

Ultrasonography demonstrated a well-defined heterogeneous lesion measuring 10.6 × 10.3 × 13.4 cm within the right scrotal sac, situated superior to the right testis (Figures *1A*, *1B*). The lesion had a heterogeneous solid-cystic echotexture with multiple variable-sized nodular components and a few calcific foci (Figure *1B*, Figure *2*). The right testis was separately visualized with preserved morphology (Figure *3*). The left testis, left epididymis, and left spermatic cord were morphologically normal. The right spermatic cord appeared mildly tortuous. A few subcentimetric bilateral inguinal lymph nodes were identified, and no significant free fluid was described within the tunica vaginalis. No significant internal vascularity was demonstrated on color Doppler examination (Figure *4*). The ultrasound impression was of a large, well-defined heterogeneous right scrotal lesion of neoplastic etiology, for which cross-sectional characterization was recommended.

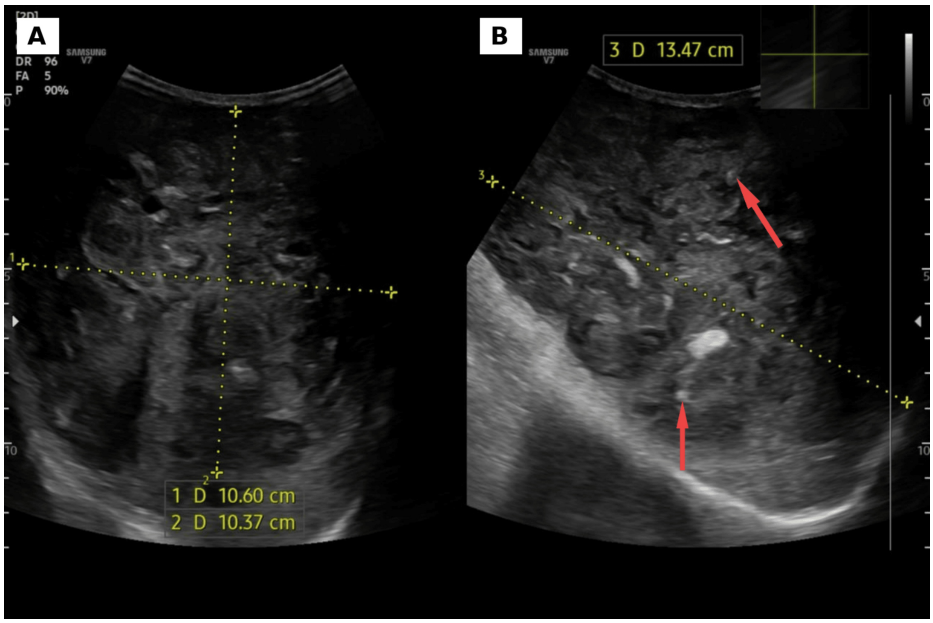


FIGURE 1: Ultrasonographic evaluation of the right scrotal mass.

(A) Grayscale ultrasonographic image of the right hemiscrotum demonstrating the anteroposterior (AP) and transverse (TR) dimensions of the lesion. (B) Grayscale ultrasonographic image demonstrating the craniocaudal dimension of the lesion. Yellow calipers indicate the respective lesion dimensions, while red arrows in (B) indicate intralesional calcific foci.

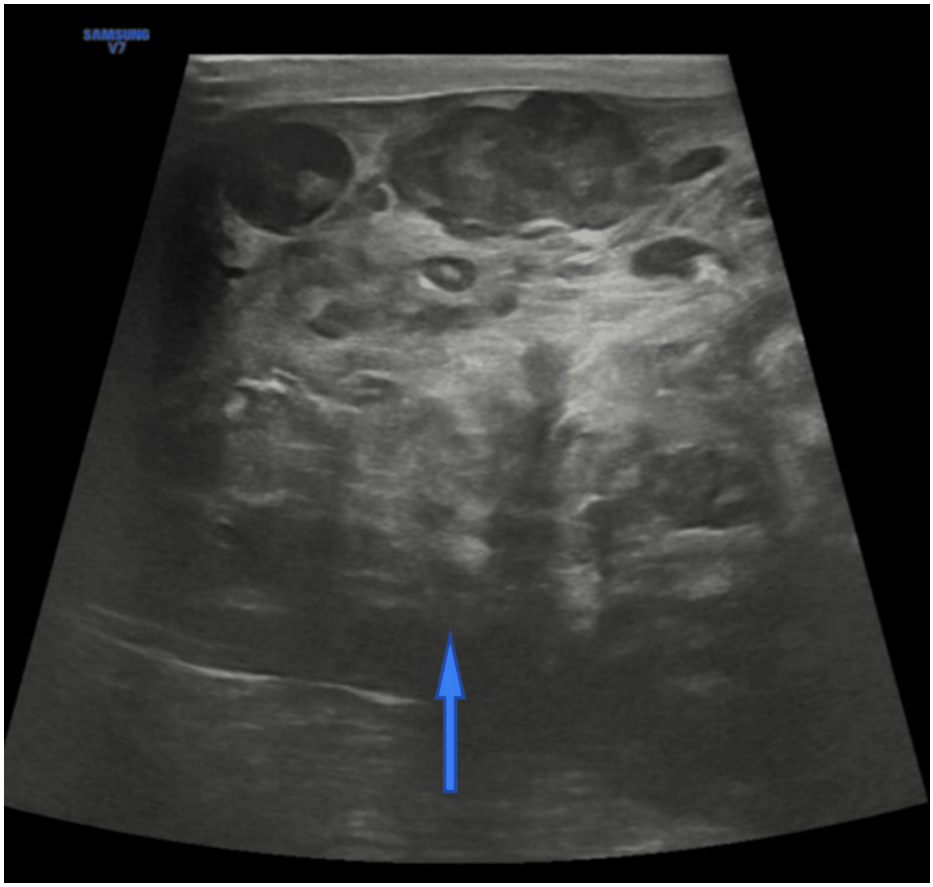


FIGURE 2: Ultrasound grayscale image demonstrating a large, well-defined heterogeneous solid-cystic lesion confined within the right hemiscrotum.

The blue arrow represents the heterogenous lesion with hyperechoic and hypoechoic areas within.

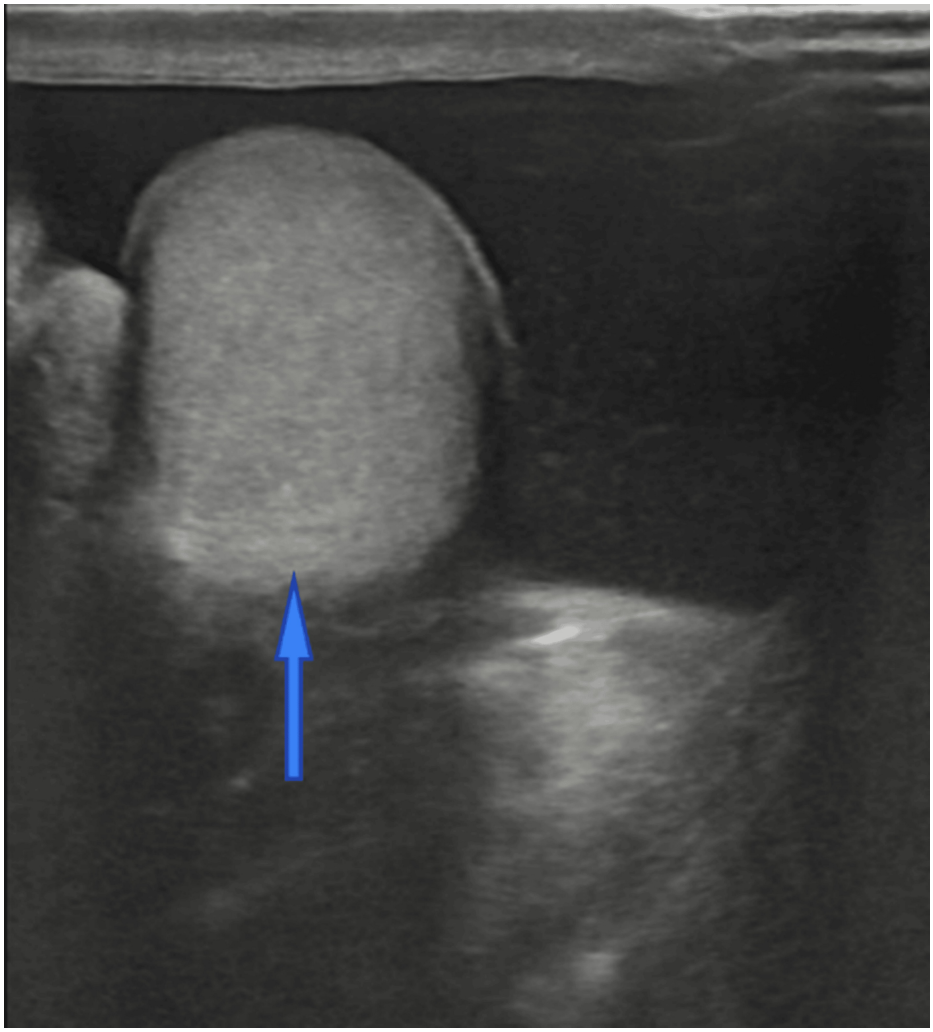


FIGURE 3: Ultrasound greyscale imaging showing the right testis separately from the lesion visualized and displaced inferiorly, supporting an extratesticular/paratesticular origin.

The blue arrow shows separate right testis with normal echopattern with minimal free fluid surrounding it.

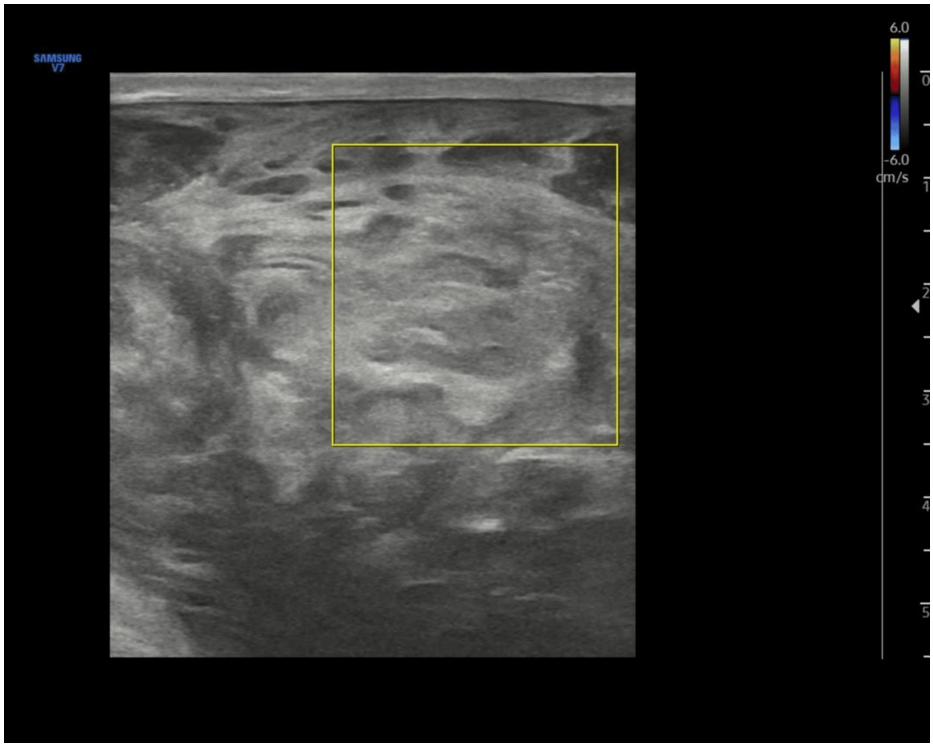


FIGURE 4: Ultrasound color Doppler demonstrating no vascularity within the lesion.

Plain CT (Figure *5*) demonstrated a large heterogeneous right scrotal/paratesticular mass occupying most of the right hemiscrotum. The right testis was separately visualized and displaced inferiorly by the mass. The right spermatic cord appeared prominent superiorly. No significant bulky regional lymphadenopathy was evident on the available examination.

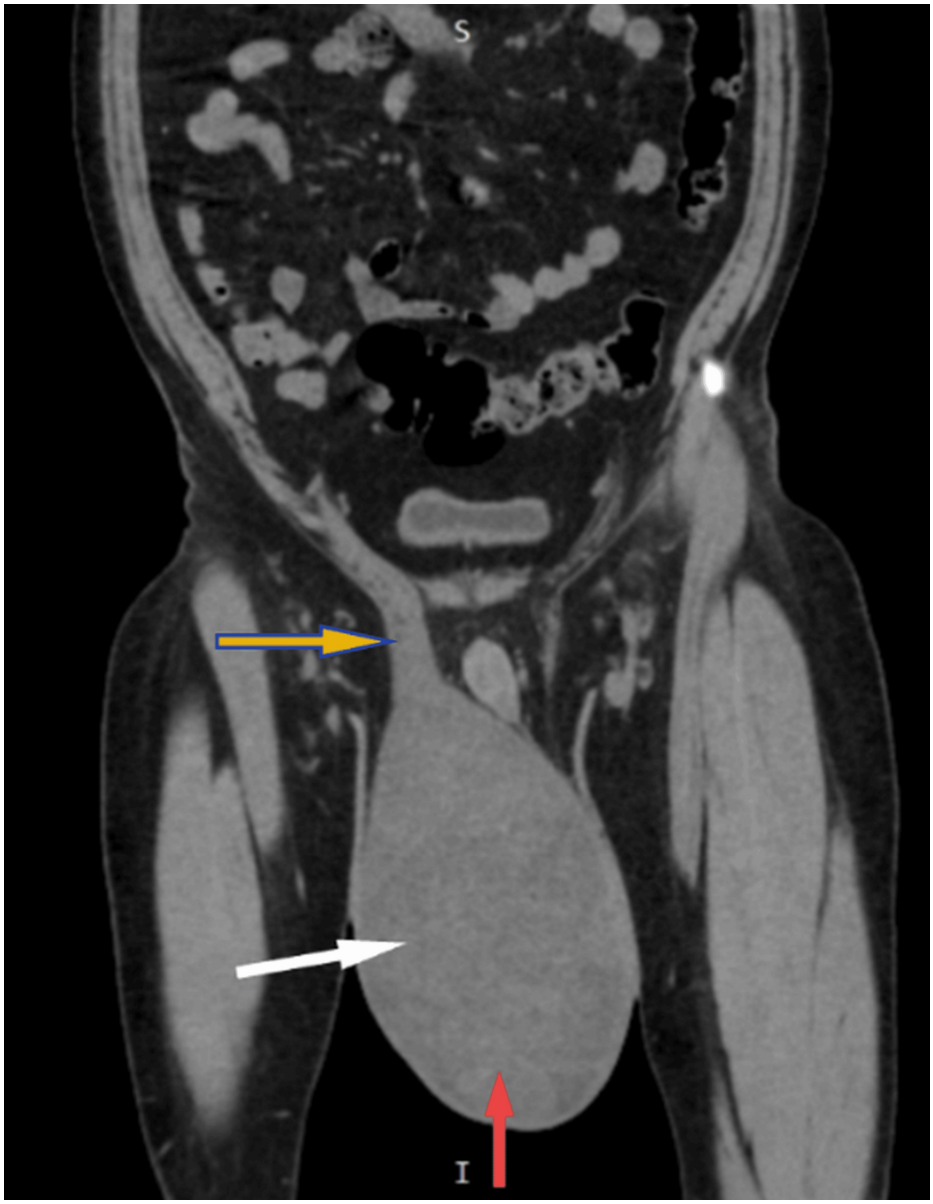


FIGURE 5: Coronal CT image of the pelvis.

Coronal CT image of the pelvis demonstrating a large heterogeneous right paratesticular/scrotal mass with inferior displacement of the separately visualized right testis and thickened right spermatic cord.

The white arrow shows the heterogeneous soft tissue density lesion in the right hemiscrotum. The red arrow shows normal density right testis noted inferiorly and separately from the lesion. The yellow arrow shows thickened right spermatic cord.

MRI of the pelvis was subsequently performed using T1-weighted, T2-weighted, short tau inversion recovery (STIR), diffusion-weighted (DWI), apparent diffusion coefficient (ADC), and susceptibility-weighted sequences, followed by multiplanar post-contrast T1-weighted imaging. A well-defined solid-cystic lesion measuring 14.6 × 11.1 × 10.5 cm was identified within the right scrotal sac. The right testis and tail of the right epididymis were separately visualized and displaced inferiorly by mass effect (Figures *6A*, *6B*). The head and body of the epididymis were not separately visualized and were considered the probable site of origin.

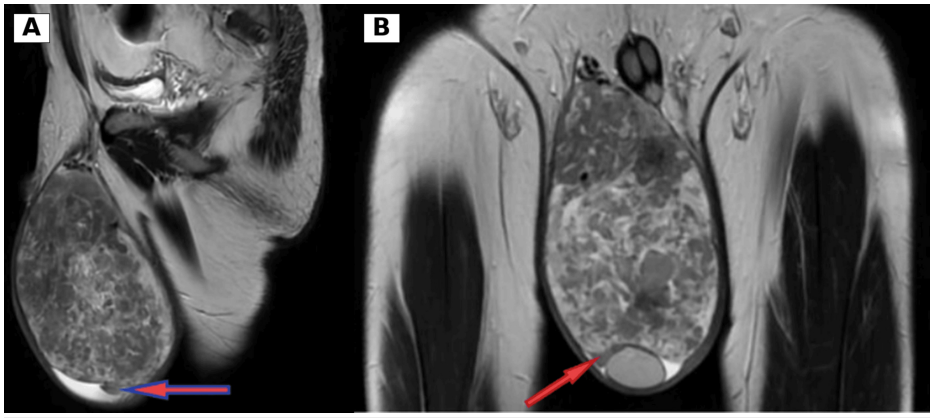


FIGURE 6: MRI findings of the right scrotal mass.

(A) Sagittal T2-weighted image and (B) coronal T2-weighted image demonstrating a large heterogeneous solid-cystic mass within the right hemiscrotum. The tail of the right epididymis is separately visualized (arrows), whereas the head and body of the epididymis are not separately visualized.

The lesion was predominantly T1 hypointense (Figure *7*), T2 and STIR hyperintense (Figure *8*), with multiple scattered hypointense solid components. Selected solid components demonstrated delayed post-contrast enhancement (Figures *9A*, *9B*). There was no convincing diffusion restriction on DWI/ADC correlation (Figures *10A*, *10B*). Susceptibility-weighted imaging demonstrated multiple tortuous linear areas of blooming corresponding to prominent intralesional vessels (Figure *11*). The right spermatic cord appeared dilated with multiple tortuous vessels and was compressed posteriorly. Superior fat planes remained preserved. The left testis was displaced toward the left by mass effect without evidence of invasion, and both testes demonstrated preserved post-contrast enhancement. Multiple small, homogeneously enhancing bilateral inguinal lymph nodes were identified, with the largest measuring 0.9 × 0.8 cm on the right. A minimal right hydrocele was present. Overall, the MRI appearance favored a benign paratesticular neoplasm. The principal imaging differentials were cellular angiofibroma and epididymal leiomyoma.

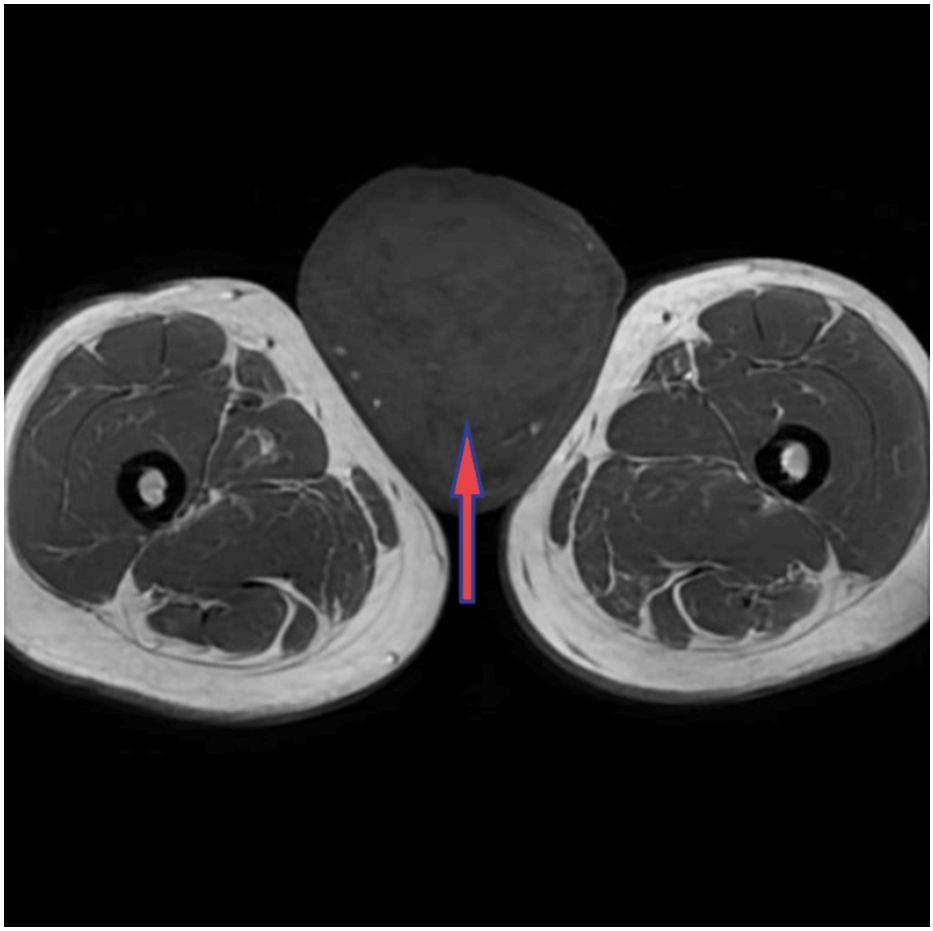


FIGURE 7: Axial T1-weighted MRI.

Axial T1-weighted image showing predominantly low-to-intermediate signal intensity lesion within the right hemiscrotum, shown by the red arrow.

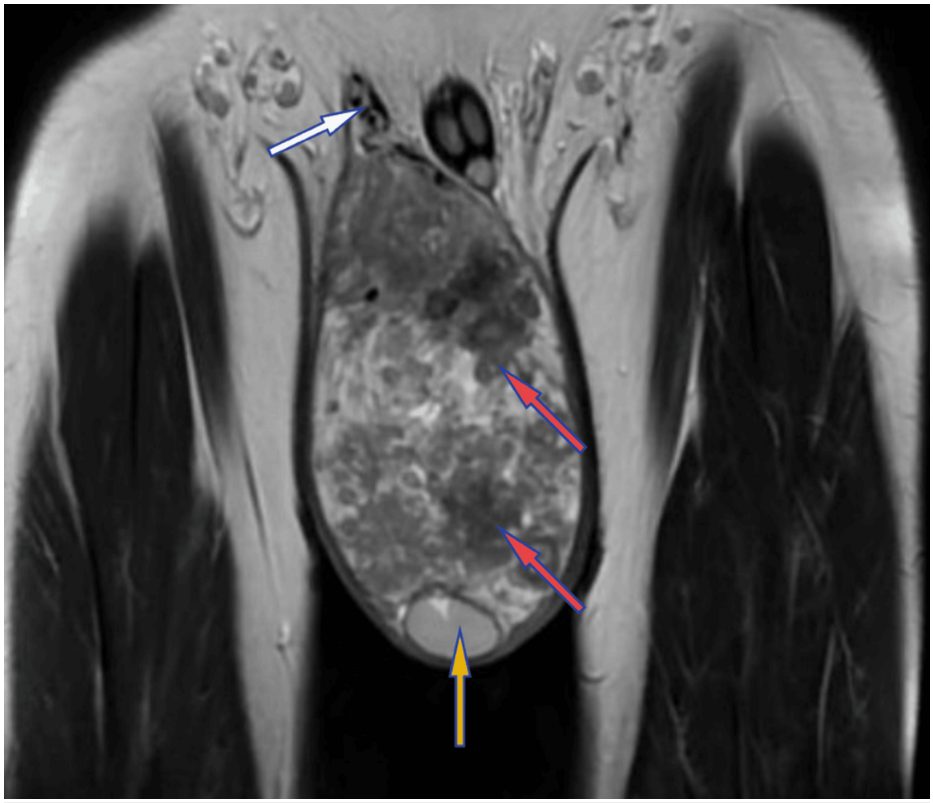


FIGURE 8: Coronal T2-weighted MRI.

Coronal T2-weighted image demonstrating heterogeneous high signal intensity within the lesion with relatively hypointense solid components.

The red arrow shows few hypointense solid components within the lesion. The yellow arrow shows separate right testis with normal signal intensity. The white arrow shows thickened right spermatic cord with few tortuous vessels noted within.

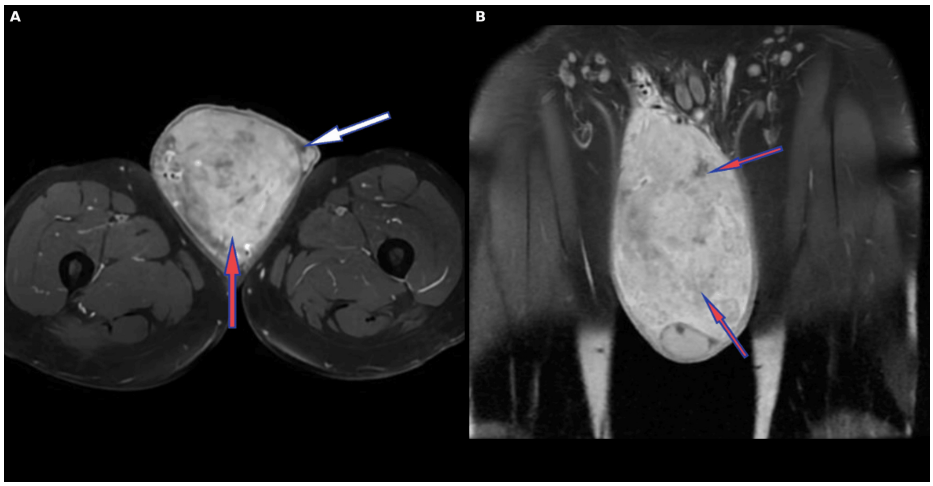


FIGURE 9: T1 post-contrast MRI.

(A) Axial post-contrast T1-weighted fat-suppressed image demonstrating heterogeneous enhancement of the solid components. The red arrow shows the heterogeneously enhancing well-circumscribed lesion in the right hemiscrotum. The white arrow shows the normal left hemiscotum. (B) Coronal post-contrast T1-weighted fat-suppressed image demonstrating the lesion-testis relationship and heterogeneous enhancement. The red arrows show the intralesional solid components that show heterogeneous delayed enhancement.

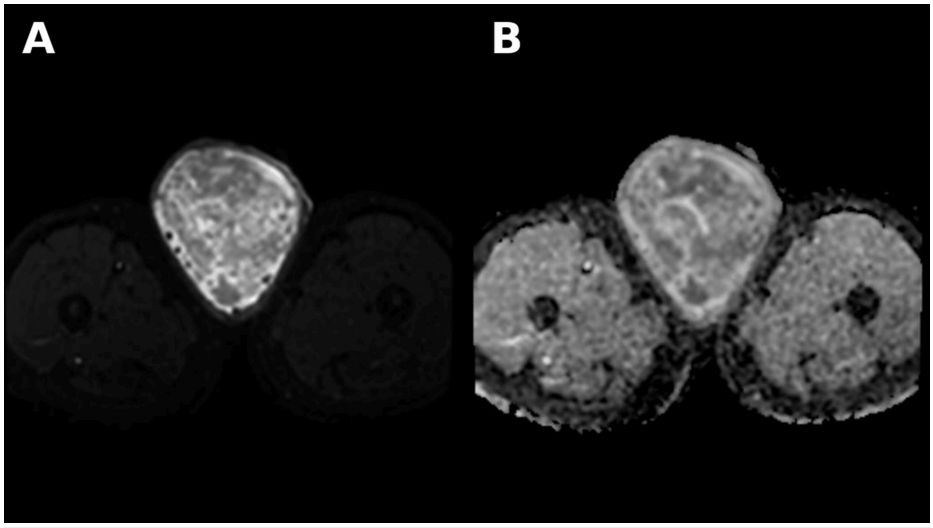


FIGURE 10: DWI and ADC images.

(A) DWI demonstrating no convincing marked diffusion restriction within the lesion. (B) Corresponding ADC map without convincing focal reduction in ADC values.

DWI: diffusion-weighted imaging; ADC: apparent diffusion coefficient

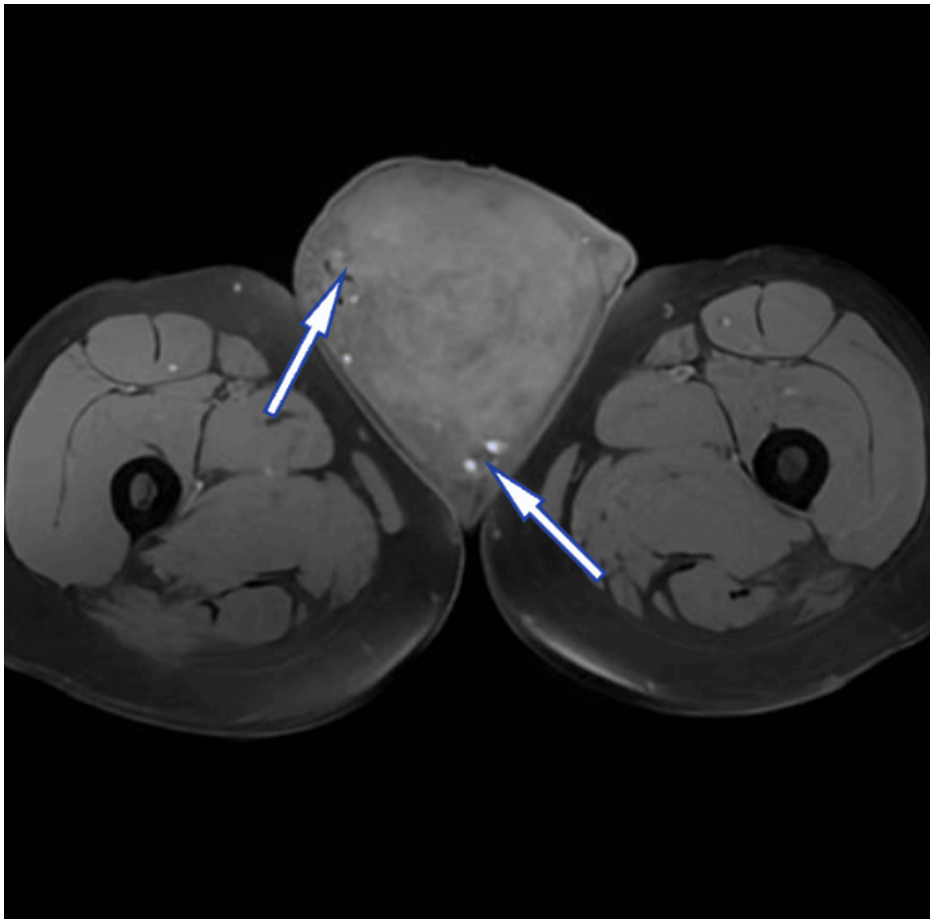


FIGURE 11: Susceptibility-weighted imaging.

Susceptibility-weighted imaging demonstrating few tortuous intralesional vascular structures (white arrows) with susceptibility blooming.

Surgical and gross pathological findings

The patient subsequently underwent radical orchiectomy for the large right paratesticular mass. The intact specimen consisted of a large paratesticular mass with an attached cord structure (Figure *12A*). The specimen weighed 850 g and measured 18.5 × 11.3 × 9.3 cm. The attached cord measured 5.7 × 1.5 cm. The external surface was bosselated with grayish-yellow discoloration. On sectioning, the tumor measured 15.0 × 9.2 cm and was predominantly whitish with a lobulated appearance. Multiple cystic spaces and vascular/hemorrhagic areas were present (Figure *12B*). The testis was separately identifiable and measured 4.0 × 2.1 cm. The gross specimen therefore correlated with the imaging findings of a large, circumscribed, heterogeneous paratesticular mass with preservation of the testis as a separate structure.

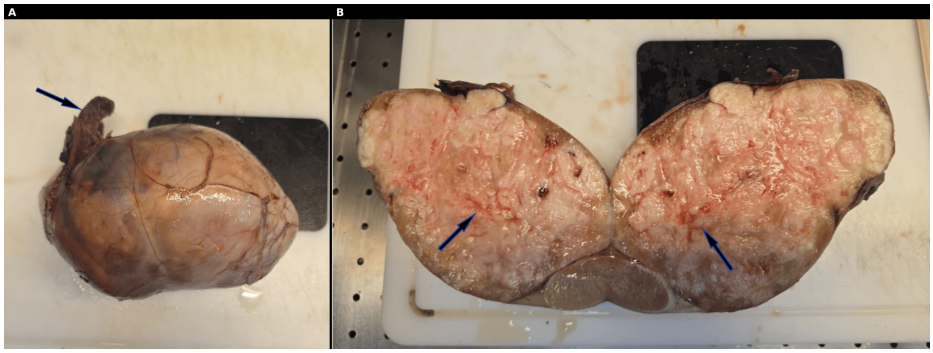


FIGURE 12: Gross findings of paratesticular leiomyosarcoma.

(A) Gross appearance of the intact paratesticular mass with attached spermatic cord (black arrow). (B) Cut surface demonstrating a large, whitish, lobulated predominantly solid mass with multiple cystic and hemorrhagic foci within (black arrows).

Histopathology

Microscopic examination demonstrated a circumscribed spindle-cell neoplasm composed of lobules of spindle cells arranged predominantly in fascicles (Figure *13A*). The tumor cells demonstrated oval to elongated, hyperchromatic and irregular nuclei, mild-to-moderate anisokaryosis, and occasional multinucleation, suggestive of mild-to-moderate nuclear atypia (Figure *13B*). Mitotic activity was recorded as 8 mitoses per 10 high-power fields (HPF). No tumor necrosis was identified. The intervening connective tissue was edematous and contained inflammatory cells and congested blood vessels.

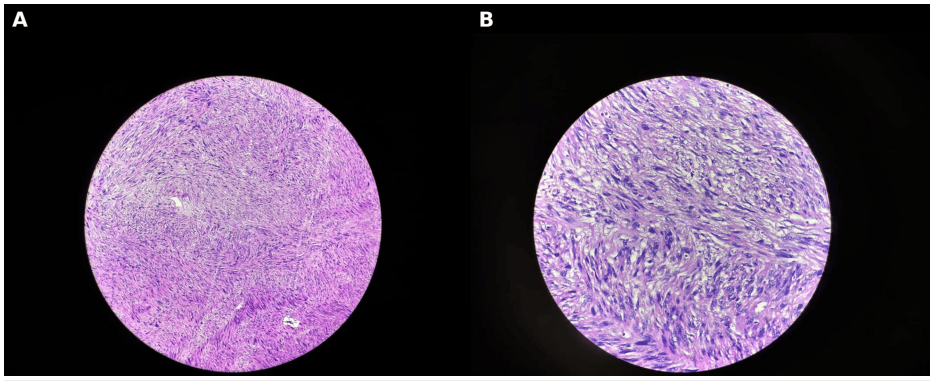


FIGURE 13: Histopathological findings of paratesticular leiomyosarcoma.

(A) Low-power hematoxylin and eosin staining showing a circumscribed spindle-cell neoplasm arranged predominantly in intersecting fascicles. (B) High-power hematoxylin and eosin staining demonstrating elongated, hyperchromatic, irregular nuclei with mild-to-moderate anisokaryosis and occasional multinucleated cells.

Immunohistochemical examination demonstrated positive immunoreactivity for smooth muscle actin (SMA) and desmin, supporting smooth muscle differentiation. The Ki-67 proliferation index was approximately 10%. Additional immunohistochemical markers, including h-caldesmon, pan-cytokeratin, S100, CD34, and STAT6, were not performed.

Histopathological grading was performed according to the French Federation of Cancer Centers Sarcoma Group (FNCLCC) grading system. The tumor differentiation score was 2, mitotic activity score was 1 (8 mitoses per 10 HPF), and tumor necrosis score was 0. The cumulative FNCLCC score was 3, corresponding to Grade 1 (low-grade) malignancy.

The separately examined testicular tissue demonstrated seminiferous tubules containing all stages of spermatogenesis, with focal atrophic changes and thickened basement membranes. Interstitial Leydig cells and thin-walled vessels were present. The cord-like structure contained blood vessels. The final histopathological diagnosis was leiomyosarcoma.

Postoperative management and follow-up

Following radical orchiectomy, histopathological assessment demonstrated complete surgical excision with microscopically negative resection margins (R0), without tumor involvement of the spermatic cord. In view of the complete resection and negative margins, adjuvant chemotherapy and radiotherapy were not recommended. However, considering the exceptionally large tumor size (18.5 × 11.3 × 9.3 cm), the patient was advised regular clinical and radiological surveillance, with follow-up imaging planned at six months postoperatively. At the time of manuscript preparation, the planned six-month follow-up period had not yet elapsed. Therefore, postoperative recurrence status and long-term oncological outcome could not be established.

Discussion

Paratesticular leiomyosarcoma is a rare smooth muscle malignancy with reported sites of origin including the spermatic cord, tunica, epididymis, and scrotal soft tissues [1,3,6]. In a classic clinicopathologic series of 24 paratesticular leiomyosarcomas, the epididymis accounted for only one tumor [1]. A subsequent systematic review identified 13 reported cases of epididymal leiomyosarcoma, with a median patient age of 66 years and reported tumor diameters generally ranging from 2 to 7 cm [4]. The size of the present tumor, therefore, represents an important feature of this case.

The clinical presentation of paratesticular leiomyosarcoma is often nonspecific, most commonly consisting of a painless or slowly enlarging scrotal or paratesticular mass [1,4]. In the present case, progressive right hemiscrotal enlargement was the principal clinical manifestation.

Ultrasonography is central to the initial evaluation of scrotal masses because it provides high spatial resolution and establishes the relationship of a lesion to the testicular parenchyma [2]. Reported sonographic appearances of epididymal leiomyosarcoma are variable. In the systematic review by Song et al., all reviewed lesions were solid, while heterogeneous echogenicity was common; where Doppler vascularity was documented, internal vascularity was described [4]. In the present case, the lesion was markedly heterogeneous and solid-cystic, but no significant internal Doppler vascularity was demonstrated. This relative lack of Doppler vascularity may have contributed to the benign-leaning interpretation.

CT has a secondary role in the initial characterization of scrotal masses but is valuable when a malignant paratesticular tumor is suspected, particularly for assessment of regional and distant disease [3,7]. Reported CT appearances of paratesticular leiomyosarcoma include heterogeneous soft-tissue attenuation, cystic or necrotic degeneration, calcification, and displacement or involvement of the spermatic cord and adjacent structures [7]. In the present case, CT confirmed the large heterogeneous paratesticular location and displacement of the testis.

MRI provides superior soft-tissue characterization and is particularly useful for determining the site of origin and relationship of a paratesticular mass to the testis, epididymis, spermatic cord, and adjacent soft tissues [2]. Paratesticular leiomyosarcoma may demonstrate variable T1 and T2 signal intensity and heterogeneous enhancement related to differences in cellularity, smooth muscle tissue, hemorrhage, and necrosis [2,7]. In this case, the lesion was predominantly T1 hypointense and T2/STIR hyperintense, with scattered hypointense solid components and delayed enhancement.

DWI deserves particular attention in this case. Restricted diffusion may be present in cellular malignant components, but diffusion characteristics are not sufficiently established to exclude leiomyosarcoma when restriction is absent. A recent epididymal leiomyosarcoma reported high DWI signal with corresponding low ADC values, in contrast to the absence of convincing diffusion restriction in the present lesion [8]. The lack of restriction in this case should therefore be interpreted as an example of imaging variability rather than as evidence of benignity.

Susceptibility-weighted imaging demonstrated prominent tortuous intralesional vessels in the present case. This finding corresponded with the congested blood vessels described histologically. Although this provides useful radiologic-pathologic correlation, the observation should not be considered a validated diagnostic feature because additional cases are required to determine whether susceptibility-related vascular findings have reproducible diagnostic significance.

The principal imaging differentials in this case were cellular angiofibroma and epididymal leiomyoma. Cellular angiofibroma is a benign mesenchymal tumor with a predilection for the inguinoscrotal region and may present as a circumscribed soft-tissue mass. Epididymal leiomyoma is also typically well circumscribed and may show variable signal characteristics when degeneration is present [2]. The probable epididymal-head location, well-defined margins, solid-cystic morphology, and absence of convincing diffusion restriction collectively favored a benign paratesticular neoplasm on MRI.

Histopathological examination remains essential for establishing the diagnosis of paratesticular leiomyosarcoma, particularly in lesions with imaging characteristics that may suggest benignity. In the present case, the spindle-cell morphology and immunohistochemical positivity for SMA and desmin supported smooth muscle differentiation. The tumor demonstrated a mitotic count of 8 mitoses per 10 HPF, with no identified tumor necrosis. According to the FNCLCC grading system, the cumulative score was 3, corresponding to Grade 1. The Ki-67 proliferation index was approximately 10%. The absence of additional immunohistochemical markers, including H-caldesmon, pan-cytokeratin, S100, CD34, and STAT6, represents a limitation of the present case and restricted further immunophenotypic characterization.

In the present case, radical orchiectomy achieved complete surgical excision with microscopically negative margins (R0), without spermatic cord involvement. Adjuvant chemotherapy and radiotherapy were not recommended following complete resection. However, considering the exceptionally large tumor size, continued clinical and radiological surveillance was advised, with follow-up imaging planned at six months postoperatively.

The principal lesson is that well-defined margins and absent diffusion restriction should not be interpreted in isolation as reliable evidence of benignity. The combination of very large size, progressive enlargement, heterogeneous solid-cystic architecture, calcific foci, prominent intralesional vessels, and degenerative or hemorrhagic components should maintain suspicion for malignancy even when local invasion is not demonstrated.

Recent reports demonstrate that paratesticular leiomyosarcoma continues to be reported across different clinical and anatomic settings, including a 2026 case involving a much smaller paratesticular mass [9,10]. The present case adds a distinct imaging perspective by documenting a giant lesion with a benign-leaning multimodality appearance, preservation of the testis as a separate structure, absent convincing diffusion restriction, and radiologic-pathologic correlation of intralesional vascularity.

Conclusions

Paratesticular leiomyosarcoma is a rare malignant mesenchymal tumor with variable multimodality imaging appearances. Ultrasound is central to establishing extratesticular origin, MRI provides detailed local characterization, and CT is primarily useful for staging. The present case demonstrates that even a giant paratesticular leiomyosarcoma may exhibit well-defined margins, solid-cystic architecture, and no convincing diffusion restriction, resulting in a benign-leaning differential diagnosis. Therefore, apparently benign imaging characteristics should not exclude malignancy in a large or progressively enlarging paratesticular mass. Definitive diagnosis requires histopathological assessment. In this case, histopathology and immunohistochemistry established the diagnosis, with FNCLCC Grade 1 classification. Complete surgical excision with negative margins was achieved, and continued postoperative surveillance was advised in view of the exceptionally large tumor size.

Additional Information

Author Contributions

All authors have reviewed the final version to be published and agreed to be accountable for all aspects of the work.

Concept and design: Anvay Pangaonkar, Pratiksha Sachani, Suresh Phatak, Kajal Mitra, Prashant Onkar

Acquisition, analysis, or interpretation of data: Anvay Pangaonkar, Pratiksha Sachani, Suresh Phatak, Kajal Mitra, Prashant Onkar

Drafting of the manuscript: Anvay Pangaonkar, Pratiksha Sachani, Suresh Phatak, Kajal Mitra, Prashant Onkar

Critical review of the manuscript for important intellectual content: Anvay Pangaonkar, Pratiksha Sachani, Suresh Phatak, Kajal Mitra, Prashant Onkar

Supervision: Suresh Phatak, Kajal Mitra, Prashant Onkar

Disclosures

Human subjects: Informed consent for treatment and open access publication was obtained or waived by all participants in this study. **Conflicts of interest:** In compliance with the ICMJE uniform disclosure form, all authors declare the following: **Payment/services info:** All authors have declared that no financial support was received from any organization for the submitted work. **Financial relationships:** All authors have declared that they have no financial relationships at present or within the previous three years with any organizations that might have an interest in the submitted work. **Other relationships:** All authors have declared that there are no other relationships or activities that could appear to have influenced the submitted work.

References

1. Fisher C, Goldblum JR, Epstein JI, Montgomery E: Leiomyosarcoma of the paratesticular region: a clinicopathologic study. Am J Surg Pathol. 2001, 25:1143-9. 10.1097/00000478-200109000-00004
2. Nicola R, Menias CO, Dahiya N, Robinson K, Hara AK, Siegel CL: Review of paratesticular pathology: findings on ultrasound and MRI. Abdom Radiol (NY). 2017, 42:585-601. 10.1007/s00261-016-0870-0
3. Jhang D, Amin K, Farkouh A, Eshaghian E, Alsyouf M, Hu B: Paratesticular tumors: a systematic review and proposed risk-based management algorithm. Urology. 2026, 207:248-58. 10.1016/j.urology.2025.08.055
4. Song R, Xi J, Shi H, Xue Z, Li H, Yu X: Ultrasonographic manifestations and the effective diagnosis of epididymal leiomyosarcoma: case report and systematic literature review. Front Oncol. 2023, 13:1101801. 10.3389/fonc.2023.1101801
5. Naimi Z, Zarraa S, Kammoun S, Yahyaoui S, Driss M, Nasr C: Primary paratesticular leiomyosarcoma: a case report and literature review. Case Rep Urol. 2020, 2020:8827214. 10.1155/2020/8827214
6. Kyratzi I, Lolis E, Antypa E, Lianou MA, Exarhos D: Imaging features of a huge spermatic cord leiomyosarcoma: review of the literature. World J Radiol. 2011, 3:114-9. 10.4329/wjr.v3.i4.114
7. Keenan RA, Nic An Riogh AU, Stroiescu A, Fuentes A, Heneghan J, Cullen IM, Daly PJ: Paratesticular sarcomas: a case series and literature review. Ther Adv Urol. 2019, 11:1756287218818029. 10.1177/1756287218818029
8. Cong Q, Liu J, Huang Z, Gao R, Zhang H, Hu J: Epididymal leiomyosarcoma: a case report . Discov Oncol. 2026, 17:299. 10.1007/s12672-026-04443-0
9. Sallay NS, Dayaratna T, Ariyaratne HL: Paratesticular leiomyosarcoma: the first reported case from Sri Lanka. Cureus. 2026, 18:e107536. 10.7759/cureus.107536
10. Munoz Pena EO, Garcia Fernandez K, Miller A, Vasquez J, Zayat V: A rare case of paratesticular leiomyosarcoma. Cureus. 2023, 15:e43294. 10.7759/cureus.43294